

The induction of preferred orientation in a liquid crystal co-polyester by extrusion and drawing

J. C. JENKINS, G. M. JENKINS

Department of Materials Engineering, University College of Swansea, Singleton Park, Swansea, SA2 8PP, UK

It is shown that liquid crystal polyester can be extruded and drawn from the melt into fine fibres which possess stiffnesses up to 68 GPa. Thicker fibres with smaller draw ratios have correspondingly lower stiffnesses, which are correlated with molecular alignments characterized by flat plate X-ray diffraction. Fibres with a range of diameters were heat-treated over a range of temperatures to determine the effect of annealing on preferred orientation and stiffness. Heat-treatment of as-spun fibres produced maxima in axial stiffness at 170°C, corresponding to an increase in preferred orientation, and 270°C, corresponding to the development of quasi-crystalline order which is analysed. Scanning electron microscopy showed the existence of needle-like domains of approximately circular cross section up to 0.8 µm in diameter. These were aligned in the direction of drawing in contrast to being haphazardly arranged in a hot rolled specimen displaying no preferred orientation.

1. Introduction

Liquid crystal or mesomorphic polyesters have been shown to yield fibres with good mechanical properties when spun either from solution [1, 2] or from the pure melt [2-4]. The directors of the component rod-like molecules tend to align easily along the fibre axis during hot stretching following extrusion. The greater the draw ratio, the more perfect is the general alignment, producing good strength and stiffness. The production of fibres from the melt is more straightforward in comparison to producing fibres from polymer solution and should therefore be more commercially attractive.

Past work by Acierno *et al.* [3] on the melt spinning of a nematic co-polyester produced by the transesterification of poly(ethylene terephthalate) and *p*-acetoxybenzoic acid has demonstrated the importance of annealing in enhancing the stiffnesses of melt spun fibres. This was imputed to an increase in crystallinity of the hydroxybenzoic acid segments on heat treatment. Shimamura *et al.* [4], working on a cholesteric cellulose derivative, reported a slight increase in preferred orientation obtained by annealing extrudates at 150°C. The 100 reflections of the wide angle X-ray diffraction patterns also appeared sharper, indicating a more crystalline structure. Other workers [5, 6] have also shown the importance of annealing.

However, annealing can also produce a decrease in preferred orientation at 300°C in a thermotropic co-polyester as reported by Donald and Windle [7]. Carbonaceous mesophase fibres derived from a refined petroleum pitch by Bright and Singer [8] have shown a decrease in the preferred orientation on gradual annealing to 500°C before a marked increase

in orientation which took place on graphitization at 3000°C with a general enhancement in mechanical properties. Recent work on extruded and stretched petroleum pitch mesophase filament has also shown a decrease in preferred orientation on heat treatment before coking at 500°C [9]. Finer filaments of such mesomorphic material with very high draw ratios show an increase in preferred orientation on heat treatment after carbonization [10]. It is, therefore, very important to choose the right heat treatment campaign to produce the best mechanical properties which are, in turn, related to the changes in molecular ordering and preferred orientation in mesomorphic fibres in general. This has been carried out here on a melt spun experimental liquid crystal co-polyester developed by ICI, Wilton.

Tharper and Bevis [11] have already demonstrated the high degree of preferred orientation in fibres produced from a similar co-polyester, whilst Donald and Windle [12] have studied the effect of annealing on structure in thin films of the co-polymer.

2. Extrusion and stretching

The extrusion apparatus consisted of an electrically heated 16 mm diameter stainless steel plunger and tube in which co-polyester could be melted and extruded through a 2 mm diameter orifice attached to the base of the tube. In a series of preliminary experiments to determine rheological behaviour, it was found that the optimum extrusion temperature required for drawing a wide range of filament diameters was 300°C. This temperature was therefore employed for all spinning operations reported here. Once the required extrusion temperature of 300°C

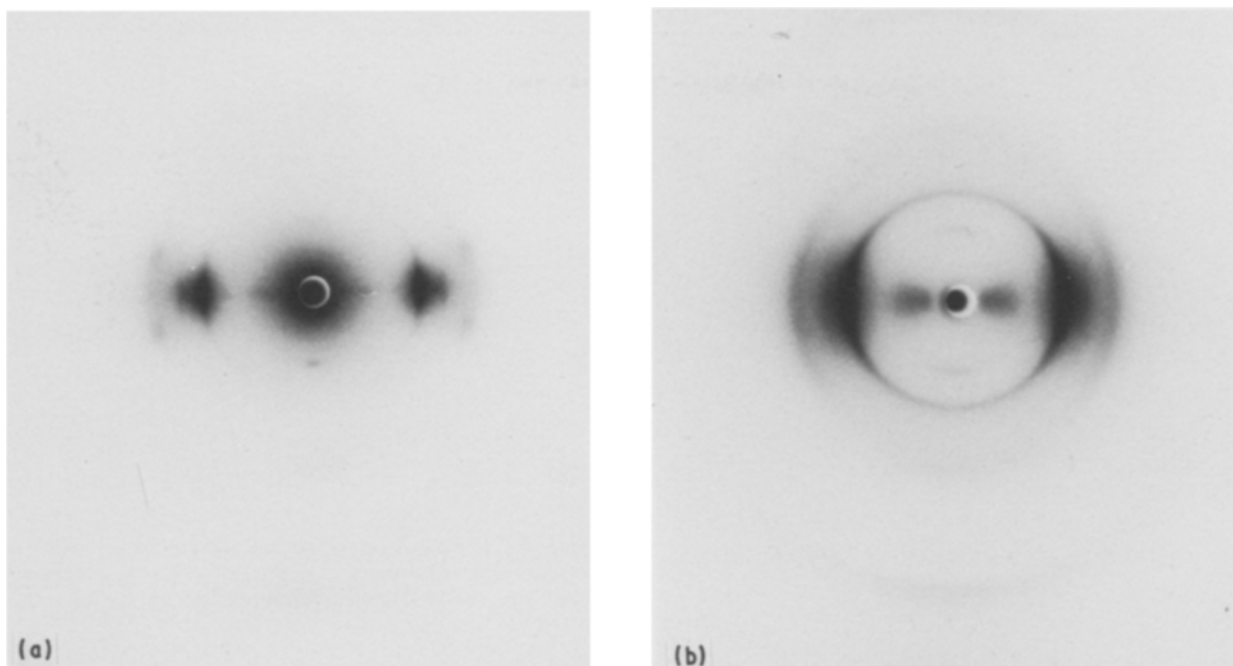


Figure 1 Flat plate X-ray diffraction patterns of (a) 200 μm diameter co-polyester fibre and (b) 1.78 mm diameter co-polyester rod. Both heat treated to 270°C.

was reached, the plunger load was increased to produce extrusion. A range of different draw ratios was obtained by pulling the extrudate away from the orifice at different rates.

Fibre specimens were annealed over a range of temperatures with 2 h at each temperature. Flat plate X-ray diffraction was carried out after each anneal in order to characterize the changes in molecular orientation relative to the fibre axis. The X-ray diffraction patterns of Figs 1a and b for 200 μm and 1.78 mm diameter specimens show how the azimuthal distribution of the planes separated at a Bragg interplanar distance of 0.448 nm depends on the fibre diameter. Both specimens in this case were annealed at 270°C. The greater amount of hot drawing in the finer 200 μm fibre produced less azimuthal spread, indicating a greater amount of preferred orientation of molecular chains in the stretching direction.

3. Hot rolling

Hot rolling was carried out to determine what effect it had on the preferred orientation of the co-polyester. The hot roller consisted of two 100 mm diameter rollers internally heated with spiral heating elements; therefore, no heat was lost during rolling which was performed on a moulded billet of co-polyester. Rolling at 320°C produced a 2.2 mm thick plate representing an 86% gauge reduction.

Figs 2a to c show flat plate X-ray diffractions of beam impingement on the longitudinal rolled edge, the transverse rolled edge and the rolled face, respectively. They indicate an absence of any preferred orientation.

4. Densitometry of the X-ray diffraction patterns

A convenient method of quantifying the preferred orientation is that of measuring the full width at half

maximum (FWHM in degrees) of the azimuthal intensity from densitometer traces around a 4 mm annulus to include all the radial broadening at the 0.448 nm reflection. $\gamma = 0$ corresponds with a horizontal line from the centre of the X-ray pattern to the right side. The raw azimuthal densitometer trace within the annulus must be corrected by subtracting the background radiation which, in highly oriented specimens, will be equal to the X-ray intensity at $\gamma = \pi/2$. A monotonic decrease in radial intensity at $\gamma = \pi/2$ confirms the absence of 0.448 nm layer planes at this orientation in Fig. 3a for the 200 μm fibre. Thus, the intensity at this point is purely due to background radiation. For the 1.78 mm specimen with much less preferred orientation, an extrapolation must be carried out as shown in Fig. 3b since the X-ray intensity at $\gamma = \pi/2$ includes some diffraction from 0.448 nm planes oriented perpendicular to the stretching direction. The total azimuthal distribution, minus the background radiation, I_b , gives the corrected azimuthal distribution $I(\gamma)$. Typical patterns for the two specimens are shown in Figs 4a and b for the 200 μm and 1.78 mm specimens, respectively.

The FWHM in degrees of $I(\gamma)$ on the X-ray plate represents not only the azimuthal X-ray intensity profile $G(\gamma)$ due to preferred orientation, but also the X-ray broadening $H(\gamma)$ due to finite domain dimensions and internal strains [9]. $I(\gamma)$ is a convolution of $G(\gamma)$ and $H(\gamma)$. However, $H(\gamma)$ may be ignored here in view of the sharpness of the meridional reflections in Figs 1a and b.

5. Preferred orientation correlated with fibre gauge and heat treatment temperature

Fig. 5 shows a linear relationship between the FWHM of $I(\gamma)$ and diameter for various 'as stretched' fibres up to 620 μm . The limiting FWHM is 10° when the line is

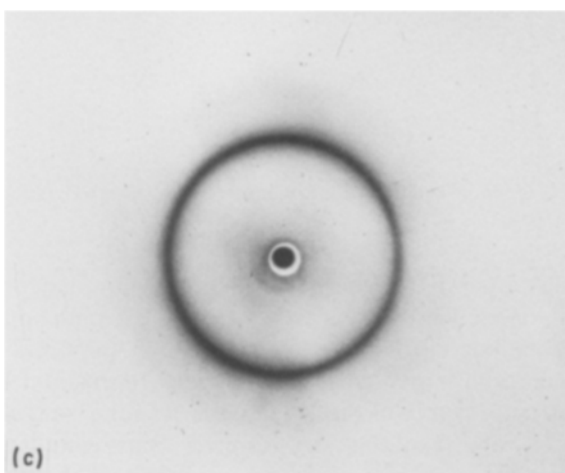
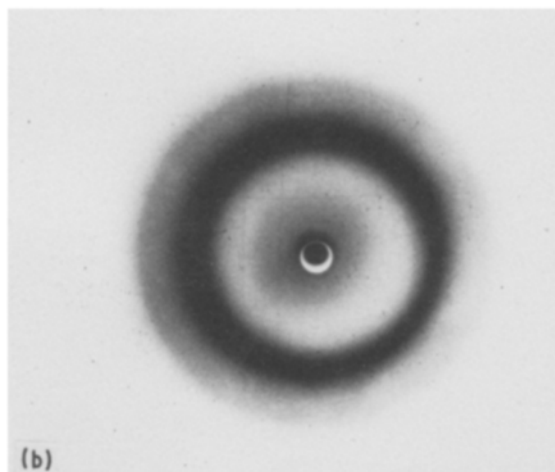
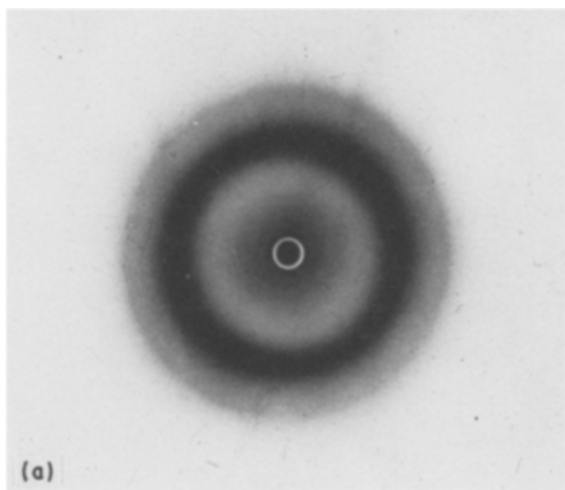


Figure 2 Flat plate X-ray diffraction patterns of hot rolled copolyester sheet with beam impingement on (a) the longitudinal rolled edge, (b) the transverse rolled edge, and (c) the rolled face.

orientation at 120°C. A marked increase in orientation occurs at 180°C in all four fibres. This temperature produces the maximum preferred orientation for the two thicker fibres of 200 and 440 μm whilst the maximum orientation for the two finer fibres of 120 and 130 μm is reached at 212°C before a marked loss on heating at 270°C.

Extruded and drawn rods of 560 and 620 μm diameter do not exhibit the same sharp increases and decreases in orientation as the thinner specimens of Fig 6a, although the thickest specimen of 1.78 mm diameter does exhibit the same characteristics at the same heat treatment temperatures with the two minima at 70 and 170°C representing maxima in preferred orientation.

These variations of $I(\gamma)$ with heat treatment temperature will be useful for comparison with the measurements of Young's modulus of fibres of various

extrapolated back to zero diameter and infinite draw ratio. The significance of this limiting angle is not clear at the moment. Figs 6a and b show the effect of annealing on FWHM of $I(\gamma)$. Fibres less than 500 μm in diameter show a slight increase in preferred orientation in most cases at 70°C followed by a loss of

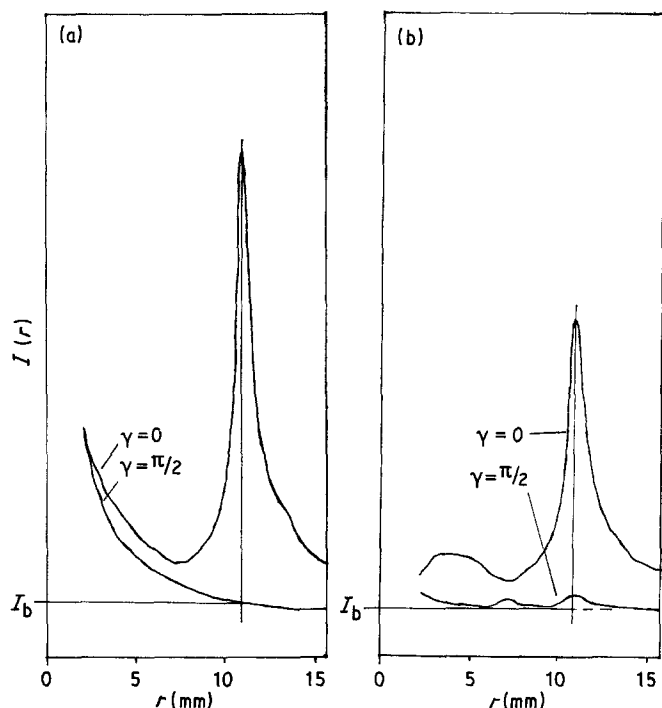


Figure 3 Radial densitometry scans of flat plate X-ray diffractions of (a) 200 μm fibre and (b) the 1.78 mm rod.

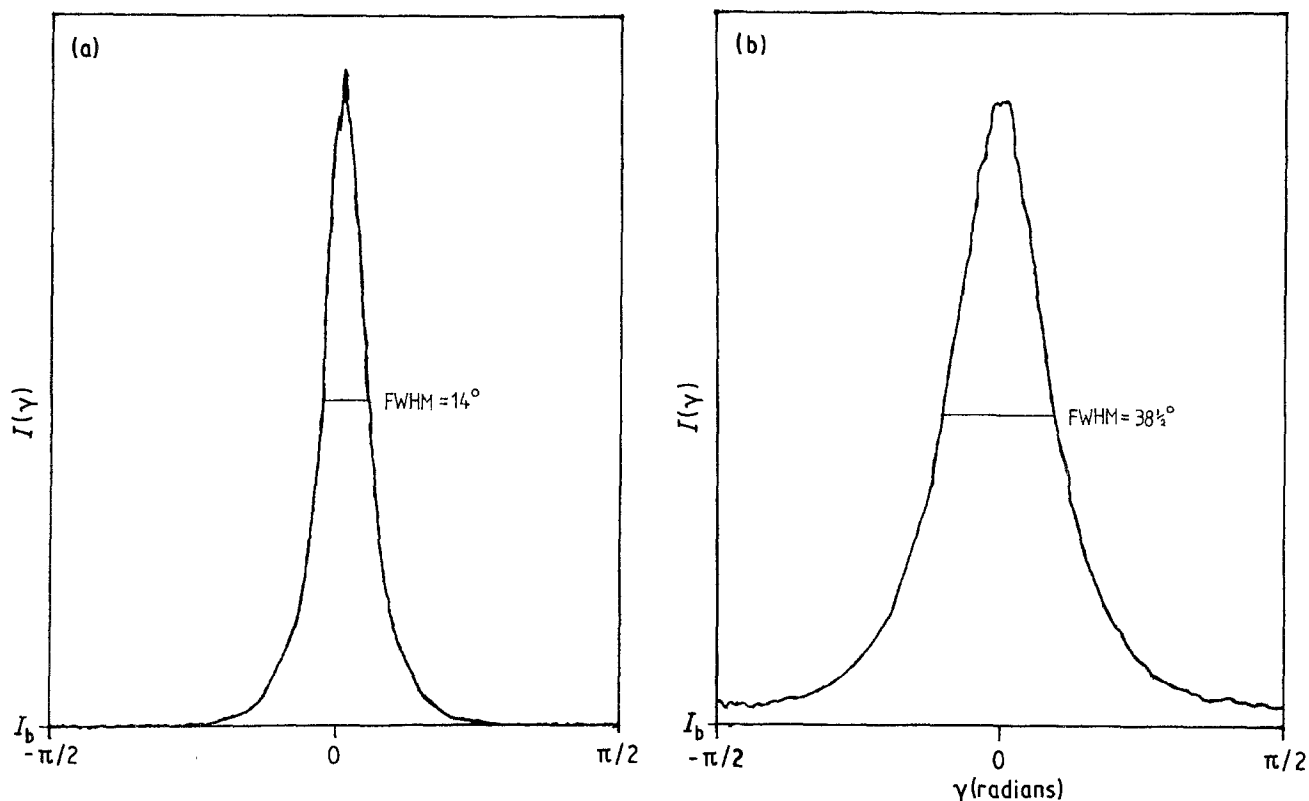


Figure 4 Azimuthal densitometry scans of (a) the 200 μm fibre and (b) the 1.78 mm rod.

diameters heat treated over the same temperature range reported later. As well as for preferred orientation analysis, the X-ray diffraction results were used to characterize the steady development of three dimensional quasi-crystalline order during annealing and slow furnace cooling; axial stiffness is related to the degree of intermolecular order as well as to the extent of preferred orientation.

The three meridional 001 X-ray reflections (with $\gamma = 90^\circ$ and 270°) (see Table I) present at all heat treatment temperatures may also be used to characterize preferred orientation, but the 0.448 nm reflection was favoured here because it appeared much stronger and was easier to analyse by densitometry.

6. The development of crystal order during annealing

Heat treatment at various temperatures up to 170°C produced more X-ray reflections as displayed in Table I, wherein the d -spacings are listed with the azimuthal angles (γ). At 220°C and below, a composite of two hkl reflections (i.e. with $\gamma = 0$ and 90°

implying $l = 0$ and h and/or $k = 0$) was evident, which at 270°C produced two well-defined hkl reflections at 0.318 and 0.329 nm demonstrating a gradual ordering process on annealing. Heat treatment at 270°C also produced another weak equatorial reflection at 1.59 nm. The overall effect is of increased ordering from a typical mesomorphic two-dimensional order to a quasi-crystalline three-dimensional order approximating to orthorhombic symmetry.

The appearance of the new reflections between 170 and 270°C is associated with a loss of preferred orientation in the very strong 0.448 nm reflection, as shown in Fig. 6a for the thinner specimens. Therefore, the gradual development of three-dimensional order between these temperatures is not necessarily associated with changes in preferred orientation which reaches a maximum in the range 170 to 212°C in all specimens as shown in Figs 6a and b. Thus the X-ray analysis shows that annealing at temperatures between 170 and 270°C should produce fibres with stiffnesses depending on the relative importances of quasicrystalline order and preferred orientation. The

TABLE I X-ray diffraction data of co-polyester

HTT	d -Spacing (nm)	Strength	Azimuthal angle (γ)	Configuration
As-annealed	0.448	S	0°	$hk0$
	0.66	W	90°	001
	0.29	W	90°	001
	0.20	W	90°	001
220°C	0.379	W	0°	$hk0$
270°C	0.397	W	0°	$hk0$
	1.59	VW	0°	$hk0$
	0.318	W	12.9°	hkl
	0.329	W	14.1°	hkl

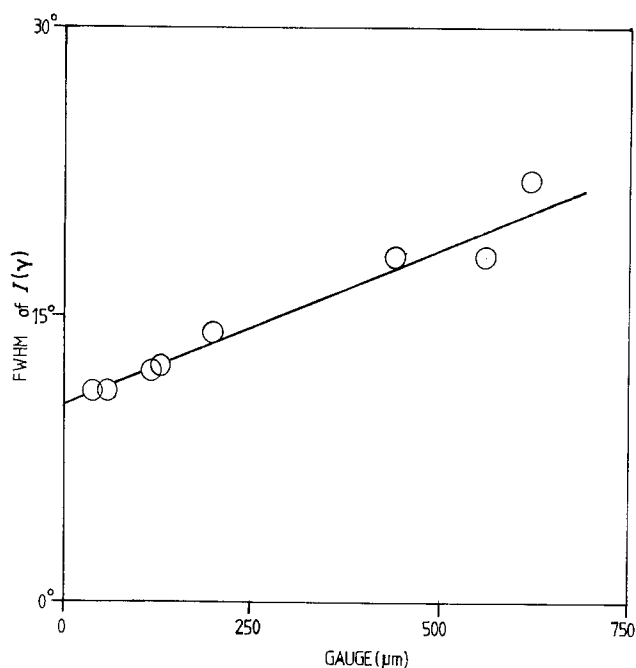


Figure 5 The preferred orientation parameter FWHM against specimen thickness.

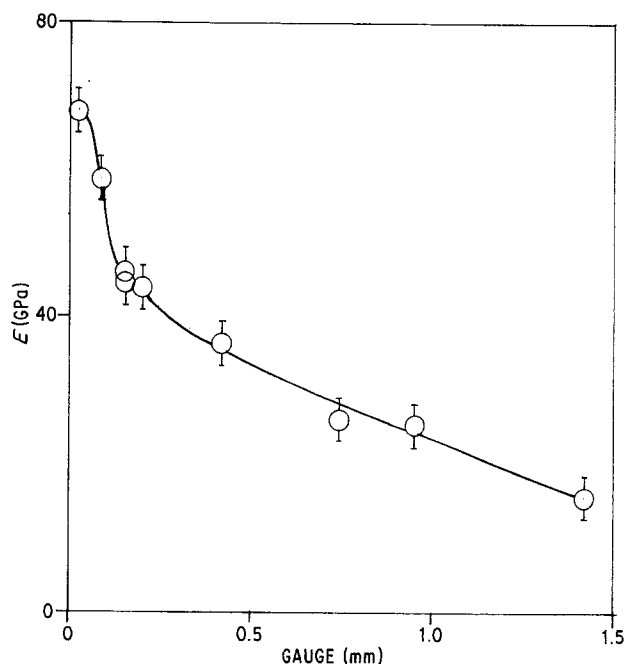


Figure 7 Young's modulus (E) against fibre gauge for specimens heat treated at 70°C .

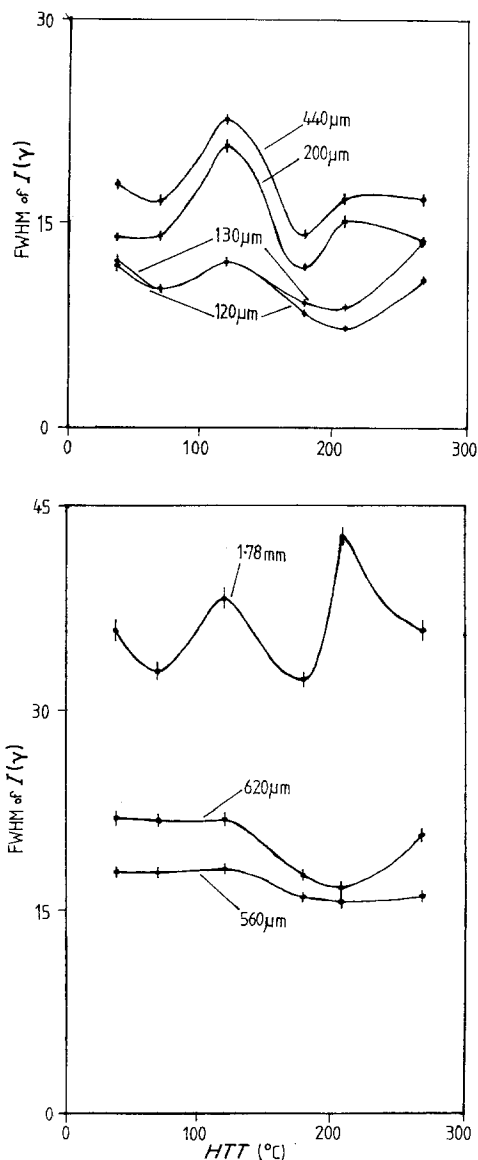


Figure 6 The FWHM of $I(\gamma)$ against heat treatment temperature for specimens (a) thinner than $500\ \mu\text{m}$ and (b) thicker than $500\ \mu\text{m}$.

variation of stiffness with heat treatment temperature will be reported in Section 8.2.

The weak but well-defined reflection at $1.59\ \text{nm}$ appearing at 270°C indicates the development of microdomains with this distinctive periodicity perpendicular to the molecular chains. Equatorial low angle scattering at all temperatures, including 270°C , over a range of d -spacing between 1.6 and $0.8\ \text{nm}$ shows how these microdomains are dimensioned perpendicular to the filament axis.

7. Dimensional stability on annealing

A $0.15\ \text{mm}$ fibre did not change length to within an accuracy of $\pm 1\%$ at any heat treatment temperature between 70 and 300°C on free end annealing. This is explained by the rigid nature of the molecules in the polyester and the absence of flexible random chain which is present in polymers like poly-aryl-ether-ketone (PEEK) which display considerable contraction during annealing [13].

8. Measurement of Young's moduli

The axial Young's moduli of fibres were measured as functions of preferred orientation, heat treatment temperature, and test temperature. Test specimens were prepared by mounting the ends of the fibres in phenolic resin. It was important to fray the ends so that the resin would grip without slip during testing. Each test specimen was heat treated at 70°C for 2 h to set the resin. This represented the minimum heat treatment temperature for the fibres. An electrically heated, double walled Pyrex chamber was constructed to fit into a tensile tester so that the testing could be carried out at elevated temperatures in clear view of the operator.

8.1. Effect of draw ratio

Fig. 7 shows the Young's moduli of a range of different fibre diameters heat treated at 70°C . The lowest

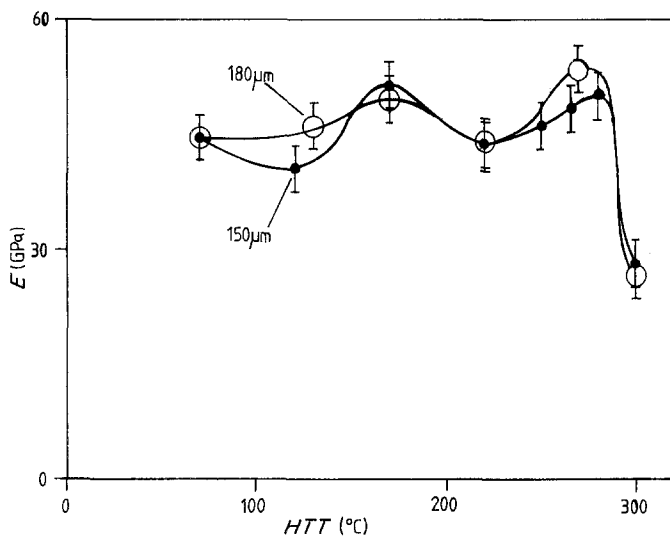


Figure 8 Young's modulus (E) against heat treatment temperature for 150 and 180 μm fibres.

modulus of 15.5 GPa for the 1.42 mm co-polyester rod corresponds with a cross-sectional area decrease factor on drawing after extrusion of 2.0 whilst a modulus of 68 GPa for the 20 μm fibre corresponds with a cross-sectional decrease factor of 10 000. Thus, the modulus is increased by a factor greater than four over this drawing range. Further decrease in filament diameter should promote further improvement in axial modulus.

8.2. Effect of heat treatment

Fig. 8 shows the effect of successive heat treatments on the stiffnesses of two fibres with each point representing heating for 2 h. The fibres were heat treated in a vacuum at 130°C and then in inert gas up to 300°C. The slight increase in stiffness between 70 and 170°C correlates well with the trends observed in the FWHM/HTT graphs of Fig. 6a over the same temperature range. The general decrease in FWHM in Fig. 6a indicates gain in preferred orientation. This implies that the stiffness should increase with heat treatment up to 170°C, as was observed.

Annealing between 170 and 220°C resulted in a decrease in stiffness which correlates well with an

increase in FWHM in Fig. 6a. Thus, any increase in three-dimensional order in this range does not compensate for the general loss in preferred orientation. By 270°C another marked increase in stiffness had occurred. This temperature produced the highest average stiffness for the two fibres and represents the optimum heat treatment corresponding with a rapid increase in ordering. It therefore appears that the development of quasi-crystalline ordering on annealing is very important in producing good stiffness. The other peak in stiffness at 170°C in Fig. 8 corresponds with maximum preferred orientation. Heat-treatment above 270°C reduces the axial modulus and this correlates with a decrease in viscosity (which is associated with randomness) as the melting temperature is reached.

8.3. Effect of test temperature

Fig. 9 shows the effect of test temperature on stiffness for a fibre 75 μm in diameter and a much thicker rod, 0.58 mm in diameter. The stiffnesses of both decrease linearly with temperature with no sign of a glass transition at 168°C in the thicker specimen. As the test temperature is raised, the Young's modulus decreases

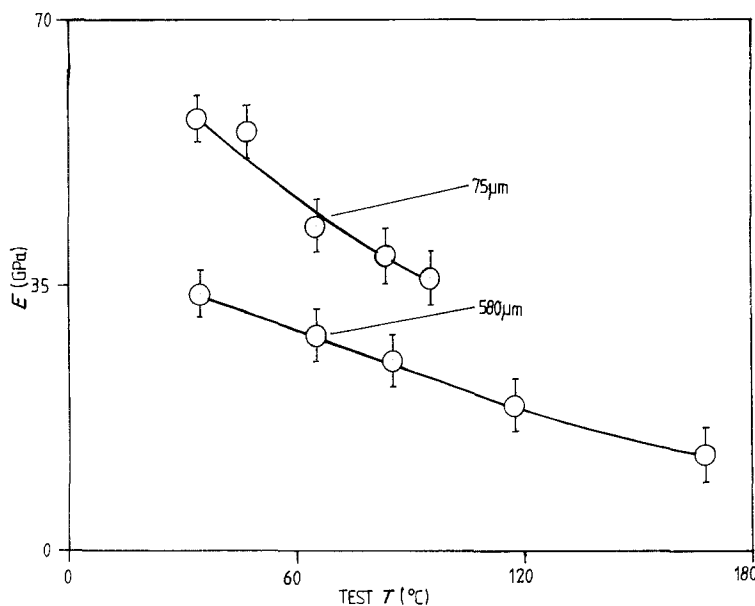


Figure 9 Young's modulus (E) against test temperature for 75 and 580 μm fibres.

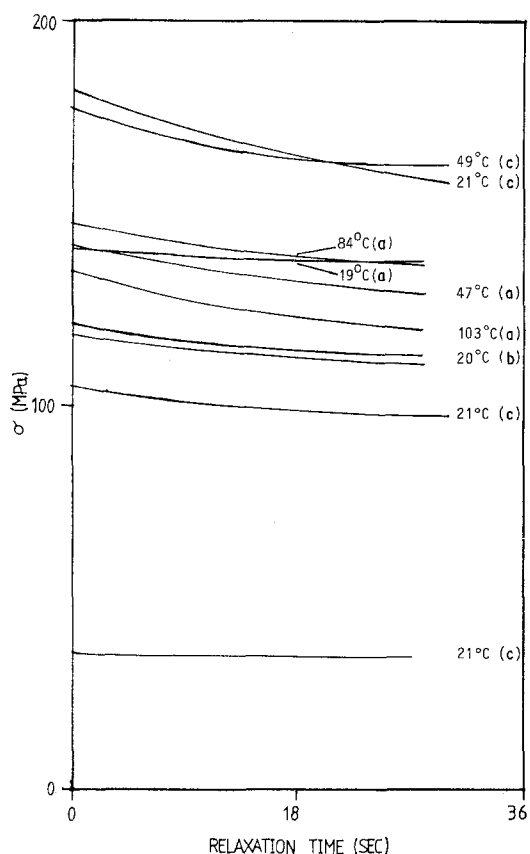


Figure 10 Stress relaxation for (a) 75, (b) 100 and (c) 200 μm diameter fibres at various test temperatures.

linearly. The proportionate rates of decrease are similar.

9. Stress relaxation

Fig. 10 shows the effect of short term stress relaxation on a range of fibres. Each fibre was taken up to the initial test stress by stretching at a rate of 0.5 mm min^{-1} . A gauge length of 30 mm was employed in all cases.

The 200 μm fibre shows negligible relaxation at an initial stress of 35 MPa at ambient temperature. Higher test temperatures and higher initial stresses resulted in much greater amounts of relaxation, as shown in Table II, for a constant relaxation time of 24 sec of constant applied strain. Comparison between the 75 μm and the 200 μm fibre at ambient temperature shows that the finer fibre was able to sustain four times the stress with only a third greater degree of relaxation $[(\sigma_{\text{max}} - \sigma)/\sigma_{\text{max}} = 0.02]$ after 24 sec.

TABLE II Stress relaxation for co-polyester fibres held for 24 sec at constant strain

Fibre diameter (μm)	Test T ($^{\circ}\text{C}$)	σ_{max}	$(\sigma_{\text{max}} - \sigma)/\sigma_{\text{max}}$	Mean rate of stress relaxation ($\text{sec}^{-1} \times 10$)
200	21	35.2	0.015	6.3
200	21	105	0.065	27.1
200	21	178	0.078	32.6
200	34	183	0.103	42.9
200	49	183	0.117	48.8
75	19	141	0.020	8.3
75	47	142	0.082	34.2
75	84	148	0.069	28.8
75	103	135	0.103	42.9

This comparison may be interpreted in terms of anisotropy of elongational viscosity. The higher the degree of preferred orientation, the higher will be the viscosity and the longer will be the time for an equal amount of stress relaxation.

10. Scanning electron microscopy (SEM)

Specimens of 280 and 145 μm diameter fibre were prepared for scanning electron microscopy. They were mounted in resin for transverse and longitudinal examination after etching in concentrated sulphuric acid for 15 min. Figs 11a to c show various aspects of the 280 μm fibre after heat treatment at 220°C whilst the fibre of Fig. 11d was heat treated at 270°C . No appreciable difference was observed in the rod-like morphology of the sub-domains shown at high magnification in Figs 11b and d over this whole temperature range to 270°C .

Fig. 11a of a transverse section shows how the sub-domains aggregate into larger anisotropic domains about 50 μm across. A U-shaped disclination can be observed in Fig. 11a indicating an eddy in the original polyester flow. A 280 μm fibre has a FWHM of 15° in the azimuthal X-ray intensity function $I(\gamma)$ according to Fig. 5. Therefore, some of the rod-like sub-domains do not appear perfectly end-on in Fig. 11b. Most of these sub-domains vary between 0.2 and 0.8 μm in mean diameter. Fig. 11c shows that they are not perfectly cylindrical. They extend over 100 μm along the length of the rod in some cases. In Figs 11b and d microfissures in the transverse section are probably caused by the etching.

Figs 11e and f of the 145 μm fibre again show the rod-like sub-domains aligned in the extrusion and drawing direction horizontal on the prints. Fig. 11g shows that some of the sub-domains can be pulled out of the transverse section by sectioning and polishing indicating higher strength within than between domains. The diameters vary from about 0.3 to 0.8 μm .

It is interesting to see how the sub-domains are arranged in a specimen in which preferred orientation is removed by hot rolling (see Section 3). Fig. 11h shows part of the transverse section of a sheet rolled at 270°C . The sub-domains appear fragmented, are clustered and are randomly arranged, in keeping with the lack of preferred orientation inferred in Figs 2a to c.

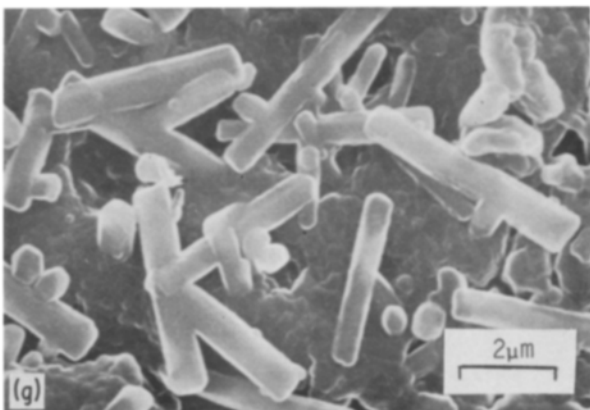
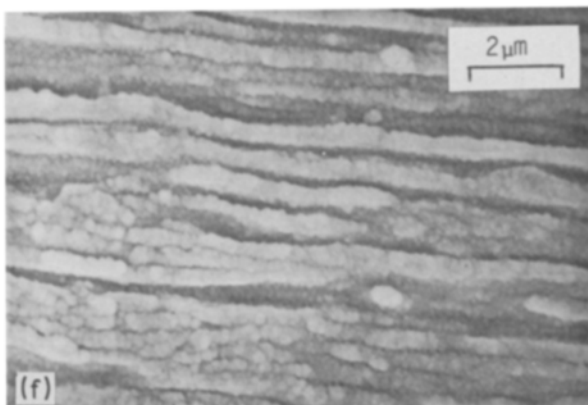
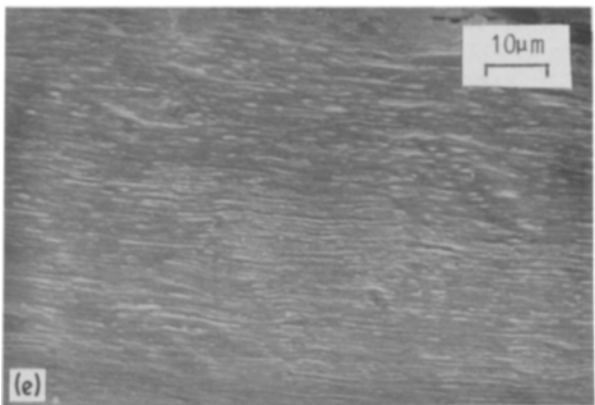
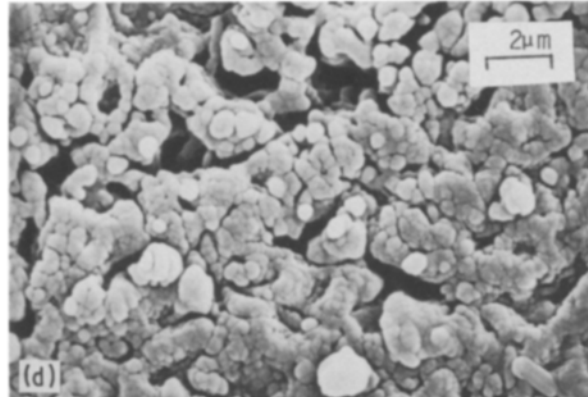
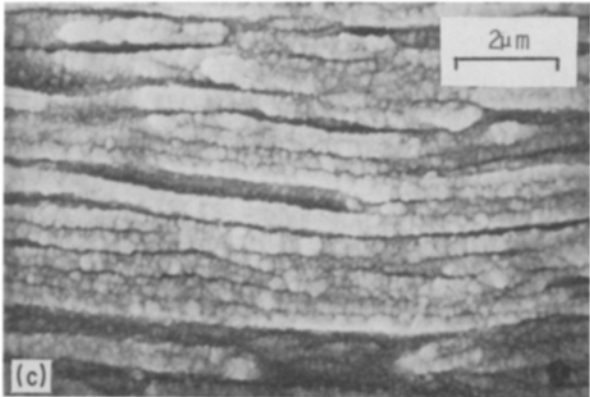
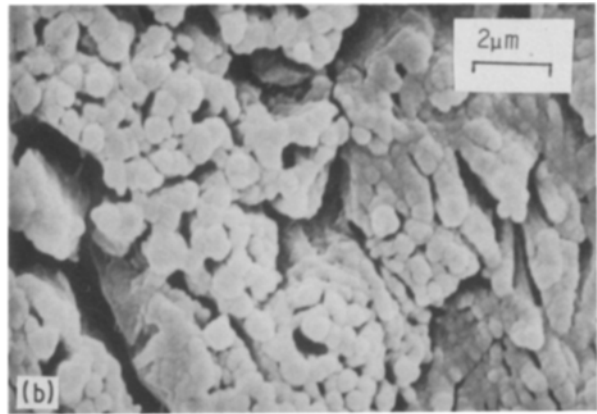
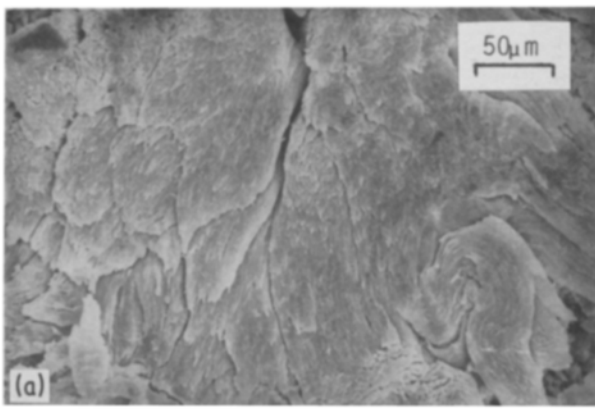


Figure 11 Scanning electron micrographs of a 280 μm fibre: (a and b) $HTT = 220^{\circ}\text{C}$, transverse section; (c) $HTT = 220^{\circ}\text{C}$, longitudinal section; (d) $HTT = 220^{\circ}\text{C}$, transverse section. SEMs of a 145 μm fibre: (e and f) $HTT = 220^{\circ}\text{C}$, longitudinal section; (g) $HTT = 70^{\circ}\text{C}$, transverse section; (h) 1.3 mm rolled sheet, transverse section.

11. Discussion

It is clear from the above observations that the stiff rod-like molecules of the co-polyester can be orientated very efficiently by simple drawing from the melt to produce high modulus fibre. The induction of preferred orientation may approximate to affine tilt deformation first proposed by Kratky [14].

The process of drawing induces the aggregation of polyester molecules into stiff and strong cylindrical domains approximately $0.5\ \mu\text{m}$ in diameter and over $100\ \mu\text{m}$ long, analogous to the microfibrils induced in long chain crystalline thermoplastics. These domains may act as distinct entities in any deformation process. Presumably, these melt above 270°C so that homogeneous flow can then take place. Below this temperature, electron microscopy indicates two phases of organized and disorganized molecules which makes the analysis of deformation using the normal assumptions of homogeneity difficult. The elastic modulus is highly anisotropic within the domains and decreases monotonically with temperature. Stress relaxation behaviour below 100°C shows a marked dependence on preferred orientation depending presumably on the ease of shear at domain boundaries.

There is no change in length on annealing in contrast to PEEK filament formed and tested under similar conditions. This shows a marked contraction on annealing [13]. Since such effects are associated with locked in strains due to the presence of lengths of flexible molecular chains, it must be presumed that such freely rotating molecular linkages are absent in the rod-like molecules of the co-polyester.

The initial drawing process presumably induces oriented 'seed' domains in a matrix of as yet unorganized material. Prolonged heat-treatment at 170°C would promote the growth of these domains and an increase in the volume of organized mesomorphic material. There would be a corresponding increase in overall preferred orientation and axial stiffness. Above this temperature some disorientation is observed, presumably in the disorganized matrix. Further heat-treatment at 270°C promotes greater inter-molecular order within the domains which would increase inter-molecular cohesion and so promote axial stiffness without further increase in preferred orientation. Just

above 270°C , the domains must melt to produce a homogeneous anisotropic fluid which can then be melt spun.

The general conclusion is that the mechanical properties of this new thermoplastic are critically dependent on both thermal and strain history and that analysis of its rheological behaviour is particularly complicated by microstructural complexities.

Acknowledgements

The authors thank Mr C. Jackson of SERC Daresbury laboratories for microdensitometry of the X-ray patterns and Mr K. Saib for help with the scanning electron micrography of the co-polyester fibres. Thanks are also due to SERC for the provision of a research grant and ICI Wilton for the provision of the co-polyester.

References

1. D. C. PREVORSEK, in "Polymer Liquid Crystals", Ch. 12, edited by A. Ciferri, W. Krigbaum and B. Meyer (Academic Press, New York, 1982).
2. A. CIFERRI and B. VALENTI, in "Ultra High Modulus Polymers" Ch. 7, edited by A. Ciferri and I. M. Ward (Applied Science, London, 1979).
3. D. ACIerno, F. R. La MANTIA, G. POLIZZOTTI, A. CIFERRI and B. VALENTI, *Macromolecules* **15** (1982) 1455.
4. K. SHIMAMURA, J. L. WHITE and J. F. FELLERS, *J. Appl. Polym. Sci.* **26** (1981) 2165.
5. W. J. JACKSON Jr and H. F. KUHFUSS, *J. Polym. Sci., Polym. Chem. Ed.* **14** (1976) 2043.
6. H. F. KUHFUSS and W. J. JACKSON Jr, U.S. Patents 3 778 410 (1973) and 3 804 805 (1974).
7. A. M. DONALD and W. H. WINDLE, *Polymer* **25** (1984) 1235.
8. A. A. BRIGHT and L. S. SINGER, *Carbon* **17** (1979) 59.
9. J. C. JENKINS and G. M. JENKINS, *ibid.* **24** (1986) 93.
10. J. C. JENKINS and G. M. JENKINS, in Proceedings of the Conference on Pitch, University of Newcastle, UK, 1987 (Society of Chemical Industry, 1987) Paper 15.
11. H. THARPAR and M. BEVIS, *J. Mater. Sci. Lett.* **2** (1983) 733.
12. A. M. DONALD and A. H. WINDLE, *J. Mater. Sci.* **19** (1984) 2085.
13. C. J. LEWIS, private communication (1986).
14. O. KRATKY, *Koll. Zh.* **64** (1933) 213.

Received 15 September 1986

and accepted 31 March 1987